

Temporally invariable bacterial community structure in the Arabian Sea oxygen minimum zone

Running page head: Invariable bacterial community structure Arabian Sea

Anand Jain¹, Mandar Bandekar¹, Jasmine Gomes¹, Damodar Shenoy², Ram Murti Meena¹, Hema Naik², Rakhee Khandeparkar¹, N. Ramaiah^{1*}

¹Microbial Ecology Laboratory, Biological Oceanography Division, CSIR-National Institute of Oceanography, Dona Paula, Goa, 403004, *Email: ramaiah@nio.org

²Chemical Oceanography Division, CSIR-National Institute of Oceanography, Dona Paula, Goa, 403004

ABSTRACT

Northeastern Arabian Sea (NEAS) is a recognized region of intense denitrification, with its 200-1200m water column being anoxic. Abundance of bacteria, viral particles as well as bacterial community (BC) were studied in addition to various chemical and other biological parameters from the Arabian Sea Time Series (ASTS) station. Water samples from surface, deep chlorophyll maximum (DCM), 250, 500 and 1000m were collected during Spring intermonsoon (SIM), Fall Intermonsoon (FIM), and Northeast monsoon (NEM) seasons and analyzed for various parameters. Bacterial abundance varied seasonally ($P \leq 0.05$), with its highest abundance observed during FIM at all sampling depths. Conversely, seasonal variations in viral abundance were minimal, though a significant correlation between virus and bacterial abundance ($r = 0.526$, $P < 0.05$, $n=14$) was evidenced. Hierarchical clustering of denaturing gradient gel electrophoresis (DGGE) profiles revealed clear patterns of vertical as well as temporal partitioning of BC during all three seasons. In that, BC varied seasonally both in the surface and DCM, whereas in the oxygen minimum zone (OMZ; 250-1000m) it was more or less identical during all three seasons in spite of significant seasonal variation in bacterial abundance, pH and DO level in the OMZ. Following the band-matching, several DGGE bands were excised and sequenced. Phylogenetic analysis of these sequences brought forth *Alphaproteobacteria*, *Gammaproteobacteria*, and *Cyanobacteria* as the dominant bacterial groups at the ASTS location. Linkage tree (LINKTREE) and canonical correspondence analysis (CCA) were performed to decipher the effect of environmental factors on the BC. From these analyses it is inferred that dissolved oxygen (DO) and total organic carbon (TOC) are responsible for vertical separation of BC between the surface and OMZ. Our results suggest seasonal variations in BC occurs in the surface layers with least or minimal temporal differences in the OMZ.

KEYWORDS: Arabian Sea . Oxygen minimum zone . Bacterial abundance . Viral abundance . Bacterial community . DGGE . CCA . LINKTREE

1. INTRODUCTION

Being the key components in the marine ecosystem, the microbial assemblages play an important role in nutrient cycling and energy flow (Azam et al. 1994, Jiao et al. 2010) and process more than half of the total primary production (Fuhrman 2002). Their biomass is often comparable to that of the phytoplankton in the euphotic zone (Simon et al. 1992). Bacterial species community composition is an important variable in most ecosystems that controls the rates and patterns of the dissolved and particulate organic matter hydrolysis. As Strom (2008) suggested, knowledge of bacterial community composition and their spatial and temporal variation is important for understanding their role in marine biogeochemistry.

Intermediate layers in some of the most productive regions of the world ocean, such as eastern tropical north pacific (ETNP, Wyrтки 1966), eastern tropical South Pacific (ETSP, Wyrтки 1966), eastern Arabian Sea (Wyrтки 1973, Madhupratap et al. 1996, Naqvi & Jayakumar 2000) and eastern South Atlantic (Bailey & Chapman 1991), are oxygen depleted. Oxygen minimum zones (OMZ) are unique habitats where organic matter is mineralized by microorganisms mostly via anaerobic processes. Typical characteristic of the OMZ is that bacteria and archaea mediate losses of fixed nitrogen to the atmosphere through denitrification (Naqvi 1994) and anaerobic oxidation of ammonia (anammox, Dalsgaard et al 2012). Although OMZ regions represent only a small fraction (~1%) of the global ocean volume (as per World Ocean Atlas 2001 (WOA01), they form an important sink for fixed nitrogen. Codispoti (2007) estimated that ocean has been losing reactive nitrogen (e.g., nitrate, ammonium and urea) through oceanic denitrification at the rate of $\sim 450 \text{ Tg N yr}^{-1}$. This reactive nitrogen in the sunlit layer limits primary production over a large expanse of the world ocean and, therefore, affects carbon sequestration. Moreover, regions of OMZ are important sources of the greenhouse gases, carbon dioxide (CO_2) and nitrous oxide (N_2O ; Naqvi et al. 1998), the latter being implicated to be also involved in the destruction of stratospheric ozone (Portmann et al 2012). In spite of the global biogeochemical and climatic importance of OMZ, many of the biogeochemical processes occurring within the OMZ, phylogenetic and metabolic diversity of the microorganisms inhabiting therein are poorly known (Riemann et al 1999; Fuchs et al 2005, Stevens and Ulloa, 2008).

The Arabian Sea is an intensely dynamic region modulated seasonally by physical forces such as upwelling, winter cooling (Prasannakumar et al. 2001) and semi-annual reversal of monsoonal winds (Madhupratap et al. 1996, Smith et al. 1998). Dramatic seasonal changes drive near-surface currents that

affect mixed-layer development, influence nutrient supply causing extremes in primary productivity patterns in this region. Consequent seasonal differences in primary production greatly influence the organic carbon concentration and flux (Hansell & Peltzer 1998). Intense mineralization of surface derived organic matter and limited supply of oxygen to intermediate waters generate prominent OMZ at intermediate depths (150-1500m; Naqvi 1994). The OMZ in the northern Arabian Sea is extremely well-developed and coincides with an extensive mid-depth denitrification (Naqvi 1994, Naqvi et al. 1998) that accounts for a third of the global marine denitrification. These changes in turn affect the abundance and distribution of bacterial communities (Ducklow 2001, Ramaiah et al. 2009, Singh & Ramaiah 2011). Over the last decade, with the advent of culture-independent methods our understanding of microbial diversity and dynamics in the Arabian Sea-OMZ (AS-OMZ) has gained impetus (Riemann et al. 1999, Fuchs et al. 2005, Divya et al. 2010, 2011). However, most studies so far from AS-OMZ mainly focused on the vertical distribution and activity of anammox bacteria (Pitcher et al. 2011), ammonia-oxidizing archeal community structure (Newell et al. 2011, Bouskill et al. 2012) and communities of nirS/nirK-type denitrifiers (Jayakumar et al. 2009, Bulow et al. 2010). Though their role in marine biogeochemistry of AS-OMZ is well-documented, effect of seasonal/environmental variations on bacterial community (BC) structure in the central Arabian Sea (CAS) region needs elucidation.

In this study, we examined the effect of seasonal variations in certain physico-chemical features and on phylogenetic composition of bacterial communities from a location in the core of AS-OMZ region through denaturing gradient gel electrophoresis (DGGE) and through cloning and sequencing of prominent, disparate bands on DGGE gels. Effects of different environmental factors on BC were assessed using multivariate analyses such as linkage tree (LINKTREE) and canonical correspondence analysis (CCA).

2. MATERIALS AND METHODS

Sample collection

Systematic sampling was carried out under SIBER program during May 2012 [Spring intermonsoon (SIM)], September 2012 [Fall intermonsoon (FIM)], and February 2013 [Northeast monsoon (NEM)]. Samples were collected during the cruises of ORV Sagar Kanya (SK-294) and of RV Sindhu Sankalp (SSK-038 and SSK-046). Seawater samples were collected using pre-cleaned Niskin bottles (washed with tap water and, rinsed with distilled water after each sampling) for bacterial abundance, viral counts, and extraction of genomic DNA at surface (0.5m), deep chlorophyll maximum (DCM that varied

between ~ 43 and 50m during seasons), intense denitrification zone (250m, 500m) and deep denitrification zone (1000m) at the Arabian Sea Time Series (ASTS) station at 17°0.126' N and 67°59.772'E (Fig. 1).

Nutrients, and dissolved oxygen measurements

For each sample, *in-situ* measurements of the physico-chemical parameters of seawater (depth, temperature, salinity, and pH) were recorded from different sensors fitted on to the CTD rosette. Dissolved oxygen (DO) was measured on-board within few hours of sampling following Winkler titration method modified by Carpenter (1965). The nutrients (nitrate, nitrite, ammonia, silicate, and phosphate) were measured from frozen samples carried to the on-shore lab in the NIO using Skalar autoanalyser (Skalar Analytical, The Netherlands) following standard methods (Grasshoff et al 1983). Values of total organic carbon (TOC) concentrations from cruises TTN043 (NEM; Jan, 1995), TTN-045 (SIM; March, 1995), and TTN-50J (FIM; August, 1995) of the Joint Global Ocean Flux Study (JGOFS) Arabian Sea Process Study (ASPS) were used from all depths we sampled during this study.

Enumeration of total bacterial cells and viral particles

Total bacterial counts (TBC) were made using a modified method of Porter & Feig (1980). In brief, subsamples of 50 ml from each depth was preserved with buffered formaldehyde (2% final concentration) and stored at 4°C in the dark until taken up for analysis. Enumeration was completed within 30 days of sample collection. One to five ml aliquots of these samples were incubated with 4',6'-diamidino-2-phenylindole (DAPI, 20µl of 1 µg ml⁻¹ working solution per ml) and filtered onto black 0.22 µm-pore-size polycarbonate membrane filters (Millipore, U.S.A). Epifluorescence microscopic counts were made using a microscope (Olympus BX-51, Japan). TBC were made from minimum of 20 randomly chosen microscopic fields from each sample to obtain a reliable mean of TBC. To obtain total numbers of viral particles, modified method of Noble & Fuhrman (1998) was followed. Briefly, one ml of seawater sample from each depth was flash frozen and store immediately at -20 °C. The samples were analyzed within 30 days after reaching NIO, Goa. Two hundred µl of the seawater sample was filtered onto 0.02 µm anodisc filter paper (Whatman, USA) under mild vacuum (< 20mm of Hg). The filter was then placed with sample side up on to a drop of SYBR Green solution for 15 min in dark. The anodisc filter was mounted on a glass slide with a drop of solution containing 50% glycerol, 50% phosphate buffered saline, and freshly prepared 0.1% p-Phenylenediamine (Sigma-Aldrich, India) on a 25 mm square cover slip to minimize the fading of fluorescence signals from the sample. Immersion oil was

placed on top of the cover-slip. Viral particles were counted in 20 randomly chosen fields under 100 X oil immersion objective of epifluorescence microscope (Olympus BX-52, Japan) using FITC filter (excitation 465/465nm, emission 515/555nm).

DNA extraction

For extraction of DNA, 2.5 L of seawater sample from each depth was passed through sterivex cartridge fitted with 0.22 μm pore size membrane filter (Millipore, USA). A peristaltic pump with 60 ml min^{-1} filtration rate was used for collecting microbial cells into the sterivex cartridge. Following this sterivex cartridge was filled with 1.8 ml of lysis buffer (50 mM Tris pH 8.3, 40 mM EDTA and 0.75 M sucrose), sealed and, stored frozen at -80°C until nucleic acid extraction was performed in the laboratory. DNA extraction was performed using modified method of Ferrari & Hollibaugh (1999). Briefly, nucleic acid extraction started with addition of lysozyme (40 μl of 50 mg ml^{-1}) and incubation of the sterivex cartridge at 37°C for 45 min. Sodium dodecyl sulfate (100 μl of 20% solution), proteinase K (100 μl of 10 mg ml^{-1}) and RNase (60 μl of 1 mg ml^{-1}) were added sequentially, and the filters were incubated at 55°C for 60 min. The lysates were purified twice by extraction with an equal volume of phenol-chloroform-isoamyl alcohol (25:24:1), and the residual phenol was removed by adding an equal volume of chloroform-isoamyl alcohol (24:1). Finally, nucleic acid was precipitated overnight in 500 μl of absolute ethanol at -20°C , followed by centrifugation at 4°C . The pellet was collected and 40 μl of TE buffer was added. The integrity of the total DNA was checked by agarose (0.8 %) gel electrophoresis. Nucleic acid extracts were stored at -80°C until taken up for further analyses.

PCR amplification

DNA extracted from all water samples collected during different seasons were subjected to DGGE-PCR, using the method described in Singh & Ramaiah (2011). In brief, variable V3 region of bacterial 16S rRNA gene was PCR amplified using DGGE specific primers, 357F-GC (5'-GCCCCGCCGCGCGCGGGCGGGGCACGGGGGGCCCTACGGGAGGCAGAG-3') and 518R (5'-ATTACCGCGGCTGCTGG-3') originally developed by Muyzer et al (1993). PCR amplification was performed using Thermocycler (Applied Biosystems, USA). The PCR mixture (50 μl) contained 1 μl of extracted DNA (5-50 $\text{ng } \mu\text{l}^{-1}$), 1 μl of each primer at a concentration of 0.5 μM , 25 μl of ReadyMix Taq PCR mix (Sigma-Aldrich, USA) [1.5 U Taq DNA polymerase; 10mM Tris-HCl, 50mM KCl, 1.5mM MgCl_2 , 0.001% gelatin, 0.2mM deoxynucleoside triphosphate (dNTP), stabilizers], and 22 μl of milliQ water. Then the DGGE-PCR was carried out with the temperature profile as follows. An

initial denaturation step of 3 min at 95°C, followed by 10 cycles of 94°C for 30 sec, 65-55°C for 30 sec (decrease by 1° After every cycle) and 72°C for 30 sec. Additional 15 cycles were allowed at the constant annealing temperature of 55°C. The final extension step was for 10 min at 72°C. In all, only 25 cycles of PCR were allowed to avoid excessive amplification of dominant fragments. However, to maximize the detection of as many ‘species’ as possible, at least three different PCR reactions were carried out for each sample. Replicate PCR products thus obtained were pooled before performing DGGE.

DGGE analysis

In order to examine the seasonal variation in BC at the ASTS, detection of DGGE bands was carried out using the D-Code universal mutation detection system as per the manufacturer’s instructions (Bio-Rad, USA). DNA concentration in the PCR products was quantified using Nano-drop (Thermo-Fisher, USA) and equal concentration of DNA per sample (~1500ng per lane) was loaded on the DGGE gel. The PCR products were resolved on 10% (w/v) polyacrylamide gel containing 30% to 60% denaturing gradient of urea and formamide for 16 hr at 60 °C at a constant voltage of 60 V in 1X TAE (40 mM tris– HCl, 20 mM acetic acid, 1 mM EDTA).The gels were stained for 30 min in 1X TAE buffer containing ethidium bromide (0.5 µg ml⁻¹), washed for 15 min and, visualized in a Gel-Doc system (Bio-Rad, USA) using Quantity One software (Bio-Rad, USA).

Analysis of DGGE profiles

Digitized DGGE gel images were analyzed with Quantity-one software (version 4.65, Bio-Rad, USA). Using rolling disk subtraction logic the software carries out a density profile analysis for each lane, detects the bands, and calculates the relative contribution of each band to the total lane intensity. Numbers operational taxonomic units (OTUs) in each sample were counted as number of DGGE bands. The bands occupying the same position in different lanes of the gel were matched with matching algorithm of the software at 1% tolerance level. Gels were cross checked visually as well for number of bands per lane. An intensity matrix was constructed based on the relative contribution of band to the total intensity of the lane. Univariate analyses were performed with PRIMER v6 software package [Plymouth Marine Laboratory, UK]. The total number of DGGE bands was used to calculate the OTU richness (S) in each sample. The relative intensity of each band (P_i) was used to calculate (a) Shannon diversity index (H') and (b) Pielou’s equitability index (J') to describe the possible changes in the dominances among DGGE-OTUs according to the following formulae:

$$H' = - \sum_{i=1}^S P_i \ln P_i \quad (a)$$

$$J' = \frac{H'}{\ln S} \quad (b)$$

Where S is the total number of OTUs and P_i is the relative intensity of the i^{th} OTU.

Though method-specific artifacts preclude its use for accurate comparative diversity analysis (Neilson et al 2013), the PCR-DGGE is still a widely used technique. Our quantitative measure of DGGE band intensities might have led to some degree of inaccuracy in diversity description. Multivariate analyses of the DGGE bands/OTUs were performed using the PRIMER v6 software package [Plymouth Marine Laboratory, UK]. The Bray-Curtis similarity index was calculated for bacterial community from five depths from all three seasons. Similarity matrix was used to perform a non-metric multidimensional scaling (NMDS) ordination and hierarchical agglomerative clustering using a group-average linking method. A similarity profile (SIMPROF) test was carried out for detecting statistically significant ($P < 0.05$) clusters (Clarke & Gorley, 2006, Clarke et al. 2008). The advantage of the SIMPROF test is that it looks for statistically significant evidence of genuine clusters of communities rather than using an arbitrary cutoff of similarity to define sample groups (Clarke et al. 2008). The SIMPROF output was superimposed on the NMDS plot in order to best reflect the formed groups.

LINKTREE analysis was performed using PRIMER v6 software package in order to find out which of the environmental parameter/s contributed to the clustering (Clarke & Warwick 2001) of BC. LINKTREE analysis helps in successive splitting of the biotic samples into two groups every time on the basis of environmental parameters. It does so using the analysis of similarity (ANOSIM) R statistic and a measure of the degree of separation of those groups in high-dimension space. ANOSIM R represents the non-parametric measure of multivariate difference between groups, rather than just a statistical test (Clarke & Warwick 2001). To relate bacterial community variation to environmental parameters, the canonical correspondence analysis (CCA) (ter Braak 1986) was performed using Multivariate Statistical Package (MVSP v3.1) software. For this analysis the environmental factors showing higher inflation of >20 were excluded, assuming colinearity of the respective variable with other variables gets included in the examined dataset.

Excision of DGGE bands and their sequencing for phylogenetic analysis

Based on their retention factor (RF) value (i.e., their position in the gel), as many as 20 DGGE bands were excised, cloned and sequenced. Before excision the bands were matched at 1% tolerance level

using Quantity-one software, and one band per set of matched bands was excised using sterile scalpel. Some unique/single bands were also excised. More importantly we did excise and sequence bands from OMZ samples as well. The excised bands were re-suspended in 40µl of MilliQ water, and stored at 4°C overnight. An aliquot (1µl) of supernatant was used for PCR re-amplification with the original primers 357F (without GC clamp) and 518 R. This yielded a fragment/product of 193 bp length. The purified PCR products were then cloned into pCR[®]4-TOPO vector (Invitrogen, USA) and transformed into *E. coli* TOP-10 competent cells according to manufacturer's instructions. Colony-PCR was used for checking the positive transformants containing appropriate size of DNA insert, using M13-20 forward and M13 reverse primers (TOPO-TA cloning guide, Invitrogen, USA), which corresponded to both sides of the cloning site on the vector. The clones were then sequenced using ABI 3130XL genetic analyzer (Applied Biosystems, USA). The sequences obtained were compared with NCBI database sequences using BLAST algorithm.

Nucleotide sequence accession numbers

Sequences obtained from excised DGGE bands were submitted to the GenBank database with the following accession numbers KF724062 to KF724081. Before submission the sequences were checked for the chimera using DISCPHER's (<http://decipher.cee.wisc.edu/>).

Statistical Analyses

Unpaired student's *t* test was performed to calculate the seasonal differences, if any, in abiotic (physico-chemical) and biotic (bacterial and viral abundance) parameters between surface layers (surface, DCM depths) and OMZ (250-1000m) depths. Single group student's *t* test was performed separately on each season data to investigate whether the bacterial, viral abundance and VBR change with depth. Repeated measures analysis of variance (RM-ANOVA) was done to check if there were seasonal differences in abiotic and biotic parameters. Linear regression analysis was performed to decipher the correlation between bacterial and viral abundances.

RESULTS

Environmental characteristics

Temperature, salinity, pH, DO and TOC were consistently higher in the surface layers than in the intense OMZ during all the three seasons. Conversely, nitrate, phosphate and silicate were significantly lower in the surface layers than in the OMZ. During NEM, higher nitrite concentrations were observed

at the DCM and 250 m (Table 1). The DO was higher in the DCM but quite low at 250m. Such distinction could not be made for the SIM and FIM seasons. Most environmental parameters analyzed during this study were significantly different (Student's *t* test $P < 0.001$) between surface layers and the intense OMZ, except nitrite and ammonia. In the surface layers, temperature ($F_{df=2} = 5.6$, $P < 0.05$), salinity ($F_{df=2} = 70.5$, $P < 0.001$), pH ($F_{df=2} = 10.54$, $P < 0.05$), silicate ($F_{df=2} = 4.8$, $P < 0.05$), and TOC ($F_{df=2} = 27.5$, $P < 0.001$) showed significant seasonal variations while (Table 1), in the OMZ such significant seasonal variation was observed only in the DO ($F_{df=2} = 6.6$, $P < 0.05$) and pH ($F_{df=2} = 38.9$, $P < 0.001$).

Bacterial and viral abundances

The lowest numbers of bacteria (out of three seasons) were recorded in the SIM season, ranging from $0.53 (\pm 0.06) \times 10^9 \text{ L}^{-1}$ in surface to $0.36 (\pm 0.02) \times 10^9 \text{ L}^{-1}$ below 250m (Fig.2A). The highest numbers, ranging from 1.4 ± 0.045 (in surface waters) to $0.6 \pm 0.03 \times 10^9 \text{ L}^{-1}$ (below 250m) were observed during FIM (Fig.2B). A secondary peak in the abundance was observed at 250m during FIM. Higher bacterial abundance was also observed during NEM, ranging from 0.8 ± 0.08 (in surface waters) to $0.57 \pm 0.07 \times 10^9 \text{ L}^{-1}$ (below 250m) (Fig.2C). Sub-surface peaks in viral abundances were also observed during SIM and FIM seasons (Fig.2A and B). RM-ANOVA brought out a significant ($P < 0.05$) seasonal variation in bacterial abundance. While seasonal variations in viral abundance across all depths were not statistically significant. A significant positive correlation between virus and bacterial abundance was evident ($r = 0.526$, $P < 0.05$, $n=14$). Single-group student's *t* test indicated significant change in bacterial abundance and Virus: bacteria ratio (VBR) with depth.

OTUs richness and diversity

The average OTU richness and Shannon diversity index (H') were statistically higher (student's *t* test $P < 0.05$) in the surface samples than in the OMZ samples (Table 2), with the highest recorded at the DCM. High Pielou's evenness index (J') (which is close to 1) was observed at all depths for all seasons, except at S-0 (Table 2).

Temporal variation in BC

Hierarchical clustering of DGGE profiles revealed clear patterns of vertical as well as temporal partitioning, with OMZ (250-1000m) profiles more closely related to one another than to surface (0-50m) profiles (Fig. 3). SIMPROF routine applied with hierarchical cluster analysis segregated the

DGGE profiles into two statistically significant clusters/groups at 5% significance level (Fig. 3). The first cluster consisted of bacterial communities residing in the OMZ (250-1000m, represented as OMZ group). The second cluster comprised profiles from (surface-DCM, represented as surface group). NMDS ordination was employed primarily to decipher similarities if any in bacterial communities temporally and/or vertically (Fig. S.1). The NMDS ordination of DGGE profiles also indicated patterns similar to those seen for hierarchical clustering analysis.

Effect of environmental parameters on BC

Similar to results from cluster (Fig. 3) and NMDS (Fig. S.1), the LINKTREE analyses that consider environmental factors (Fig. 4) also indicated similar division of bacterial assemblages/ BC. The order in LINKTREE analysis is as follows. The first split (A) separated bacterial assemblages into two groups on the basis of high pH (>8.04; left branch) or low pH (<8.02; right branch) with analysis of similarity (ANOSIM) $R = 0.74$, and absolute measure of group differences (B %) = 91. Similarly, the second split (B) separated OMZ profiles from that of the surface and is characterized by DO >200 μM but <11.8 μM) with $R=0.53$ and $B\%=61$. Alternatively, the same splitting of samples was obtained when we chose TOC >77.2 μM but <54.2) or Nitrate <0 μM but >15.3 μM or Silicate <3.08 μM but >18.5 μM . Details of such possibilities are shown in figure (4) legend. The third split (C) further segregated OMZ BC in two sub-groups due to pH <7.31 but > 7.73; $R=0.57$; $B\%=46$) and the fourth split (D) separated the surface samples in two distinct groups on the basis of TOC (>72 μM but <69.5 μM) or pH (<8.05; >8.1); $R=0.75$; $B\%=66$). From the LINKTREE analysis it is therefore possible to indicate that DO, TOC, nitrate, and silicate are equally responsible for vertical partitioning of BC into two clusters, i.e. surface and OMZ group. However, the global BEST test implied that DO and TOC are the most significant parameters (Spearman's rank correlation (ρ) =0.488 at 0.5% significance level) affecting the overall structure of BC in the ASTS location.

The CCA further confirmed the results of LINKTREE. The sum of all Eigen values (Table 3) indicated an overall variance of 0.858 in the dataset. The first two ordination axes of CCA, accounted for 32.2% of the explained total variance. The variation of the species–environment relation explained by the first two axes was 57.5%. Biplot scalings of CCA with inter-sample distances are shown in fig (5). The first canonical axis accounted for 21.7% of total explained variance and reflected strong gradient caused by DO ($R= 0.890$), pH ($R= 0.828$) and TOC ($R= 0.718$). CCA indicate that among the 10 different parameters, pH, DO and TOC seem to separate the BC into surface and OMZ communities. Further,

pH and TOC explain the temporal variations of BC in the surface waters (Fig. 5). Other environmental parameters (temp, salinity, phosphate) with high inflation ratio (>20) were excluded from both LINKTREE and CCA analyses.

Phylogenetic analysis of DGGE bands

Out of the 20 band sequences, nine affiliated to *Alphaproteobacteria*, five to *Cyanobacteria*, three to *Gammaproteobacteria*, and one each to *Deltaproteobacteria*, *Betaproteobacteria* and *Bacteroidetes* (Table 4). Based on DGGE band sequences (represented as sequences), a phylogenetic tree was constructed to compare their affiliation to the sequences in NCBI database (Fig. 6). Most of the sequences matched very well (similarity of ~98% or more) with the uncultured marine bacteria, except one sequence (B18) that matched with a sequence reported from freshwater lake. Several sequences (B1, B2, B3, B4, B5) fall within the oxygenic phototrophic group which includes *Cyanobacteria*. Their corresponding bands in the DGGE gel were found only in the samples collected from surface layers. Most sequences of *Alphaproteobacteria* (B7, B9, B11, B12, B13, B14, and B17) were found both in surface as well as OMZ. An exception was the sequence B10 (uncultured SAR-11 *alphaproteobacteria*) which was exclusively found at the surface. All *Gammaproteobacteria* sequences were found both in surface as well as OMZ, except B8 (*Pseudoalteromonas*) which is found only at the surface. The only sequences B15 (*Desulfobacterales*) affiliated to the *Deltaproteobacteria* was found exclusively in the OMZ.

The percentages of different bacterial groups based on the intensity of DGGE bands indicate dominance of *Alphaproteobacteria* and *Gammaproteobacteria* both in surface layers and OMZ during all three seasons (Fig. S.2). These bacterial clusters presented different proportions among the three seasons (Fig. S.2). In surface layers, the average percentage of *Gammaproteobacteria* increased two fold from NEM (13.1%) to SIM (25.7%) whereas *Cyanobacteria* increased four-fold from SIM (3.45%) to NEM (12.05%). Interestingly, the contribution of *Alphaproteobacteria* to surface BC did not vary much between seasons. Notably, clear seasonal variations in the percentages of *Gammaproteobacteria*, *Alphaproteobacteria* and *Deltaproteobacteria* in OMZ were not evident.

DISCUSSION

The DO concentrations in the intermediate depths/OMZ of the ASTS varied seasonally, with the lowest recorded during NEM compared to those during SIM and FIM as reported by de Sousa et al. (1996) earlier. In the NEAS, higher surface productivity (Bhattathiri et al. 1996) together with sluggish renewal

of intermediate waters (Naqvi et al. 1990) leads to intense oxygen depletion during winter season. The surface waters were devoid of nitrate during the intermonsoon periods (SIM and FIM) and quite low ($0.006 \mu\text{M}$) during NEM. During intermonsoon period, the NEAS experiences intense solar heating and is characterized by weak winds that stratify the surface layer (Muraleedharan & Prasannakumar 1996). This stratification leads to depletion of nutrients/nitrate in the upper euphotic zone. However, convective mixing facilitates the upward pumping of nutrient-rich subsurface layers during winter (Prasannakumar & Prasad, 1996), which in turn lead to high primary production. From the observations of Sen Gupta et al. (1976) it is possible to suggest that higher nitrite and least DO concentrations observed during NEM at intermediate depths (250m) may signify an intense denitrification process while the presence of nitrite in the thermocline region, the nitrification process.

Bacterial abundance varied seasonally, with the lowest and the highest recorded during SIM and FIM, respectively. The SIM is a transition period from winter to summer and is generally known to be a period of low primary productivity caused by water column stratification and oligotrophic conditions (Madhupratap et al, 1996). During this period, bacterial abundance is mainly sustained by the slow-to-degrade dissolve organic carbon (DOC) from earlier phytoplankton bloom of NEM (Ramaiah et al. 2000). Typically, bacterial abundance is more at the end of the southwest monsoon (SWM) in September (FIM). The decay of earlier, SWM phytoplankton bloom and increased exudation and/or particle breakdown at the end of the season (Ducklow 1993) would also lead to facilitation of prolongs bacterial proliferation well into FIM. The presence of a secondary peak in bacterial abundance at 250 m during FIM, is similar to earlier reports (Ramaiah et al 2005), but was not observed during other seasons. We may have missed the secondary peaks in other two seasons since our sampling depth intervals were wider. High bacterial abundance observed during NEM is unusual (Fig.2C). There is no evidence so far of a strong response of bacteria to the Northeast (NE) monsoon despite enhanced primary production and higher phytoplankton biomass. Thus, our observation might imply that during NEM bacteria respond to increased primary productivity (Bhattathiri et al. 1996). Other than high bacterial abundance observed during NEM, the seasonal trends of bacterial abundance at ASTS compare quite well with earlier data from the central Arabian Sea (Ducklow et al. 2001, Ramaiah et al. 1996, 2005).

At the ASTS location, viral abundances were an order of magnitude higher than those of bacteria, as also reported from elsewhere earlier (Wilhelm & Suttle, 1999, Alonso et al 2001, Breitbart et al. 2002). In fact, our estimates of viral counts range from 10^6 to 10^7 ml^{-1} similar to those reported earlier from

other open ocean samples by Proctor & Fuhrman (1990), Fuhrman & Suttle (1993) and, Parsons et al. (2011). These counts are much higher than those reported from the oligotrophic Alboran Sea (Alonso et al 2001) and, are comparable to those reported from Eastern Tropical South Pacific (ETPS) OMZ (Cassman et al 2012). It may be mentioned here that all counting procedures for viruses in particular are reliable for an “estimate” only. For instance, Alonso et al (2001), who compared a variety methods, point out differences in the estimates arrived by using disparate methods. As we examined the flash frozen and -20 °C stored samples our counts could be, to some extent, underestimates. However, these results are useful for a general comparison between open ocean and OMZ regions elsewhere. Subsurface peaks in viral abundances observed during SIM and FIM seasons may be due to viral induction events as Cassman et al. (2012) propose. Shedding of eukaryotic viruses (Rhodes et al. 2008) could also lead to such higher counts. Viral abundance did not vary seasonally unlike that of bacteria. This could be taken to imply that their abundance is not necessarily regulated by the biogeochemical settings and/or, their host range in the ASTS location may be broader.

Hierarchical clustering and NMDS analysis show that seasonal variation in BC mostly occurs in the surface layers with least or minimal temporal differences in the OMZ despite of the significant seasonal changes in bacterial abundance, pH and DO concentration in the OMZ. Higher Shannon diversity index (H') in the surface layers compared to that in the OMZ (Table 2) is similar to those reported earlier by Zaikova et al. (2010), Bryant et al. (2012). Competition, environmental filtering and other microbial community assembly drivers across the oxygen gradient might be responsible for such differences between the surface and OMZ communities. We speculate that, lower energy availability in the OMZ due to lower redox potentials and less readily available organic matter (refractive) govern the selection and preponderance of a few phylotypes of bacteria. Based on single observations Bryant et al (2012) and Stewart et al (2012) noted microbial communities from different depths within the OMZ to cluster together but those from surface layers quite disparate. In this regard, our study is noteworthy, since such clustering together among the OMZ BC is a perennial phenomenon in the ASTS. Dissolved oxygen, organic matter and pH, are considered key factors driving the changes in microbial community composition in aquatic ecosystems (Lindstrom & Bergstrom 2005, Haukka et al. 2006, Stevens & Ulloa 2008). However, little is known on the effects of these environmental factors on BC in the Arabian Sea, though its composition (Riemann et al 1999; Fuchs et al 2005) and functional gene diversity (Jayakumar et al. 2009, Bulow et al. 2010) from the AS-OMZ are reported. Our use of both LINKTREE and CCA for deciphering the relationship between BC and various environmental factors suggest that DO and

TOC are the major factors influencing the BC in the ASTS region. However, it is to be noted that TOC decrease with depth (Hansell and Peltzer 1998), no matter when it was measured. Therefore, the relationship we see between BC and TOC would also have been observed with samples collected at any time. Thus, TOC may be co-varying with depth but not a controlling variable.

Sequencing of DGGE bands though only 20 of them, revealed that bacterial community in the ASTS was dominated by *Alphaproteobacteria* and *Gammaproteobacteria*, as reported earlier from a variety of pelagic marine environments (Giovannoni & Rappé 2000) including OMZ of ETSP (Stevens & Ulloa 2008) and Southern Arabian Sea (Fuchs et al. 2005). Notable variation in the percent of different bacterial groups was observed in the surface layers than in the OMZ. Higher percentage of *Gammaproteobacteria* was observed in the surface layers during SIM compared to the other two seasons. Phylotypes affiliated with *Gammaproteobacteria* include *Pseudoalteromonas*, *Idiomarina*, and uncultured *Gammaproteobacteria*. The genus *Pseudoalteromonas* has often been found in close association with marine eukaryotic hosts (Holmström & Kjelleberg 1999) and known for producing agarolytic enzyme involved in the algal tissue degradation activities (Ivanova et al. 2002).

Recent studies by McCarren et al (2010) indicate the involvement of *Alteromonadales* (specifically *Idiomarina* spp. and *Alteromonas macleodii*) in metabolizing semi-labile high molecular weight dissolved organic matter (HMWDOM) to methanol or formaldehyde, and carbon dioxide. In addition to these, another group of bacteria which contributed to the variation in the surface ASTS-BC was affiliated to the genus *Flavobacteria* of Phylum *Bacteroidetes*. These are often coupled to the primary production in the photic zone and are especially proficient in degrading polymeric organic matter (Kirchman 2002). Occurrence/detection of *Bacteroidetes* during SIM and FIM might be taken to indicate the availability of high molecular weight, semi-labile polymeric organic matter during these seasons. Higher percentage of *Cyanobacteria* during NEM also contributed to the variation in surface BC. Upward pumping of nutrient-rich subsurface layers during NEM is likely to facilitate such higher abundance of *Cyanobacteria* during this period.

Contribution of *Alphaproteobacteria* to the surface and OMZ BC did not vary much with the seasons. The phylotypes affiliated with *Alphaproteobacteria* found in this study include *Rhodobacterales*, *Sphingomonadales* and members of SAR11 clade. The *Rhodobacterales* and members of SAR11 group are known to limit the flux of sulfur from the ocean by demethylating dimethylsulfoniopropionate (DMSP), which is usually degraded to the volatile dimethyl sulfide (Moran et al. 2003, Howard et al.

2006). Demethylated DMSP can serve as substrate in sulfur oxidation in the deeper layer. Interestingly, sequence B15 exclusively found at AS-OMZ was affiliated with the order *Desulfobacterales* (sulphate-reducing bacteria) of *Deltaproteobacteria* group. Similar sequences have been retrieved from below 200 m (Riemann et al. 1999, Fuchs et al. 2005). Sulfate reducing bacteria can survive under suboxic conditions (Santegoeds et al. 1998, Minz et al. 1999) and can play an important role in the cryptic sulfur cycle in the OMZ (Canfield et al. 2010). Fuchs et al (2005) speculate that at certain times and locations, specific bacterial populations might catalyze sulfate reduction and sulfide oxidation in the water column of the Arabian Sea.

The fact that, we did not find known denitrifying bacteria in our samples is a bit aberrant. Such absence of amplicons affiliated to denitrifying bacteria in the samples has been reported earlier by Stevens & Ulloa (2008) in ETPS-OMZ and by Riemann et al (1999) in AS-OMZ. Since denitrifying bacteria are widely distributed in the OMZ and they ought to be present in the study area (Jayakumar et al. 2009). Our DGGE band excising ought to have excluded many phylotypes. DGGE is a useful technique for monitoring the dynamics of a microbial community and comparison of multiple samples (Liu et al 2012). It provides gross insights on phylogenetic diversity information and only predominant populations in the assemblage (Muyzer et al. 1993). We ascertain that predominant players in the ASTS BC have been covered by our applying the DGGE technique.

CONCLUSIONS

The factors governing BC in the Arabian sea-OMZ were studied. The results indicate clear temporal variation in the surface BC mainly resulting from the seasonally induced variation in the quantity as well as quality of the organic matter. The least or minimal variation in the OMZ BC despite differences in the bacterial abundance, pH, DO level indicates temporal homogeneity and to some extends seasonal predictability of BC at the AS-OMZ.

Acknowledgements

The authors thank Director Dr SWA Naqvi, for coordination, support and encouragement. The authors thank the SIBER program of the MoES and CSIR funded project PSC0206 for the financial support. We are grateful for many valuable suggestions by the reviewers for improving the manuscript. This is NIO contribution number.....

LITERATURE CITED

- Alonso MC, Jimenez-Gomez F, Rodriguez J, Borrego JJ (2001). Distribution of virus-like Particles in an Oligotrophic Marine Environment (Alboran Sea, Western Mediterranean). *Microb Ecol* 42: 407-415.
- Azam F, Steward GF, Smith DC, Ducklow HW (1994) Significance of bacteria in carbon fluxes in Arabian Sea. *Proc Indian Acad Sci (Earth Planet Sci)* 103: 341-351
- Bailey GW, Chapman P (1991) Short-term variability during an anchor station study in the southern Benguela upwelling system – chemical and physical oceanography. *Prog Oceanogr* 28: 9-37
- Bhattathiri PMA, Pant A, Sawant, S, Gauns M, Matondkar GP, Mohan Raj R (1996) Phytoplankton production and chlorophyll distribution in the eastern and central Arabian Sea in 1994–1995. *Curr Sci* 71: 857-862
- Breitbart M, Salamon P, Andresen B, Mahaffy JM, Segall AM, Mead D, Azam F, Rohwer F (2002) Genomic analysis of uncultured marine viral communities. *Proc Natl Acad Sci USA* 22: 14250-14255
- Bryant JA, Stewart FJ, Eppley JM, Delong EF (2012) Microbial community phylogenetic and trait diversity declines with depth in a marine oxygen minimum zone. *Ecology* 93: 1659-1673
- Bouskill NJ, Eveillard D, Chien D, Jayakumar A, Ward BB (2012). Environmental factors determining ammonia-oxidizing organism distribution and diversity in marine environments. *Environ Microbiol* 14: 714-729
- Bulow SE, Rich JJ, Naik HS, Pratihary AK, Ward BB (2010) Denitrification exceeds anammox as a nitrogen loss pathway in the Arabian Sea oxygen minimum zone. *Deep-Sea Res Part I* 57: 384-393
- Canfield DE, Stewart FJ, Thamdrup B, De Brabandere L, Dalsgaard T, Delong EF, Revsbech NP, Ulloa O (2010) A Cryptic Sulfur Cycle in Oxygen-Minimum-Zone Waters off the Chilean Coast. *Science* 330: 1375-1378
- Carpenter JH (1965) The Chesapeake Bay Institute technique for Winkler dissolved oxygen method. *Limnol Oceanogr* 10: 140-143
- Cassman N, Prieto-Davó A, Walsh K, Silva GG, Angly F, Akhter S, Barott K, Busch J, McDole T, Haggerty JM, Willner D, Alarcón G, Ulloa O, DeLong EF, Dutilh BE, Rohwer F, Dinsdale EA (2012) Oxygen minimum zones harbour novel viral communities with low diversity. *Environ Microbiol* 14: 3043-3065
- Clarke KR, Gorley RN (2006) *PRIMERv6: user manual/tutorial*. Plymouth, UK: PRIMER-E.
- Clarke KR, Warwick RM (2001) *Change in marine communities: an approach to statistical analysis and interpretation*. 2nd edition. Plymouth, UK: PRIMER-E.
- Clarke KR, Somerfield PJ, Gorley RN (2008) Exploratory null hypothesis testing from community data: similarity profiles and biota–environment linkage. *J Exp Mar Bio Ecol* 366: 56-69
- Codispoti LA, Brandes JA, Christensen JP, Devol AH, Naqvi SWA, Pearl HW, Yoshinari T (2001) The oceanic fixed nitrogen and nitrous oxide budgets: Moving targets as we enter the anthropocene? *Scientia Marina* 65: 85-105

- Codispoti LA (2007) An oceanic fixed nitrogen sink exceeding 400 Tg Na⁻¹ vs the concept of homeostasis in the fixed-nitrogen inventory. *Biogeosciences* 4: 233-253
- Dalsgaard T, Thamdrup B, Farias L, Revsbech NP (2012) Anammox and denitrification in the oxygen minimum zone of the eastern South Pacific. *Limnol Oceanogr* 57: 1331-1346
- De Sousa SN, Dileep Kumar M, Sardesai S, Sarma VVSS, Shirodkar PV (1996) Seasonal variability in oxygen and nutrients in the central and eastern Arabian Sea. *Curr Sci* 71: 847-851
- Divya B, Soumya, KV, Nair S (2010) 16S rRNA and enzymatic diversity of culturable bacteria from the sediments of oxygen minimum zone in the Arabian Sea. *Antonie van Leeuwenhoek* 98: 9-18
- Divya B, Parvathi A, Loka Bharathi PA, Nair S (2011) 16S rRNA-based bacterial diversity in the organic-rich sediments underlying oxygen deficient waters of eastern Arabian Sea. *World J Microbiol Biotechnol* 27: 2821-2833
- Ducklow HW 1993. Bacterioplankton distributions and production in the northwestern Indian Ocean and Gulf of Oman, September 1986. *Deep-Sea Res II* 40: 753-771
- Ducklow HW, Smith DC, Campbell L, Landry MR, Quinby HL, Steward GF, Azam F (2001) Heterotrophic bacterioplankton in the Arabian Sea: basin wise response to year round high primary productivity. *Deep-Sea Res II* 48: 1303-1323
- Ferrari VC, Hollibaugh JT (1999) Distribution of microbial assemblages in the Central Arctic Ocean Basin studied by PCR/DGGE: analysis of a large data set. *Hydrobiologia* 401: 55-68
- Fuchs BM, Woebken D, Zubkov MV, Burkill P, Amann R (2005) Molecular identification of picoplankton populations in contrasting waters of the Arabian Sea. *Aquat Microb Ecol* 39: 145-157
- Fuhrman JA, Suttle C (1993) Viruses in marine planktonic systems. *Oceanography* 6: 51- 63.
- Fuhrman JA (2002) Community structure and function in prokaryotic marine plankton. *Anton Leeun Int J G* 81: 521-527
- Grasshoff K, Ehrhardt E, Kremling K, (1983) *Methods of Seawater Analysis*, 2nd ed., Verlag Chemie, Weinheim, p 401
- Giovannoni S J, Rappé M (2000) Evolution, Diversity and Molecular Ecology of Marine Prokaryotes. In Kirchman D (eds) *Microbial Ecology of the Oceans*. John Wiley & Sons, Inc, New York, p 47-48
- Hansell DA, Peltzer ET (1998) Spatial and temporal variations of total organic carbon in the Arabian Sea. *Deep-Sea Res II* 45: 2171-2193
- Haukka K, Kolmonen E, Hyder R, Hietala J, Vakkilainen K, Kairesalo T, Haario H, Sivonen K (2006) Effect of nutrient loading on bacterioplankton community composition in lake mesocosms. *Microb Ecol* 51: 137-146
- Holmstrom C, Kjelleberg S (1999) Marine Pseudoalteromonas species are associated with higher organisms and produce biologically active extracellular agents. *FEMS Microbiol Ecol* 30: 285-293

Howard EC, Henriksen JR, Buchan A, Reisch CR, Buergmann H, Welsh R, Ye W, González JM, Mace K, Joye SB, Kiene RP, Whitman WB, Moran MA (2006) Bacterial taxa that limit sulfur flux from the ocean. *Science* 314: 649-652

Ivanova EP, Sawabe T, Alexeeva YV, Lysenko AM, Gorshkova NM, Hayashi K, Zukova NV, Christen R, Mikhailov VV (2002) *Pseudoalteromonas issachenkonii* sp. nov., a bacterium that degrades the thallus of the brown alga *Fucus evanescens*. *Int J Syst Evol Microbiol* 52: 229-234

Jayakumar A, O'Mullan GD, Naqvi SWA, Ward BB (2009) Denitrifying bacterial community composition changes associated with stages of denitrification in oxygen minimum zones. *Microb Ecol* 58: 350-362

Jiao N, Herndl GJ, Hansell DA, Benner R, Kattner G, Wilhelm SW, Kirchman DL, Weinbauer MG, Luo T, Chen F, Azam F (2010) Microbial production of recalcitrant dissolved organic matter: long-term carbon storage in the global ocean. *Nature Reviews Microbiol* 8: 593-599

Kirchman DL (2002). The ecology of *Cytophaga-Flavobacteria* in aquatic environments. *FEMS Microbiol Ecol* 39: 91-100

Liu M, Xiao T, Wu Y, Zhou F, Huang H, Bao S, Zhang W (2012) Temporal distribution of bacterial community structure in the Changjiang Estuary hypoxia area and the adjacent East China Sea. *Environ Res Lett* 7 025001: 11

Lindstrom E, Bergstrom A (2005) Community composition of bacterioplankton and cell transport in lakes in two different drainage areas. *Aquat Sci* 67: 210-219

Madhupratap M, Prasannakumar S, Bhattathiri PMA, Kumar MD, Raghukumar S, Nair KKC, Ramaiah N (1996) Mechanism of the biological response to winter cooling in the northeastern Arabian Sea. *Nature* 384: 452-549

McCarren J, Becker JW, Repeta DJ, Shi Y, Young CR, Malmstrom RR, Chisholm SW, DeLong EF (2010) Microbial community transcriptomes reveal microbes and metabolic pathways associated with dissolved organic matter turnover in the sea. *PNAS* 107: 16420-16427

Minz D, Fishbain S, Green SJ, Muyzer G, Cohen Y, Rittmann BE, Stahl DA (1999) Unexpected population distribution in a microbial mat community: sulfate-reducing bacteria localized to the highly oxic chemocline in contrast to a eukaryotic preference for anoxia. *Appl Environ Microbiol* 65: 4659-4665

Moran MA, Gonzalez JM, Kiene RP (2003) Linking a bacterial taxon to sulfur cycling in the sea: studies of the marine *Roseobacter* group. *Geomicrobiol J* 20: 375-388

Muyzer G, de Waal EC, Uitterlinden AG (1993) Profiling of complex microbial populations by denaturing gradient gel electrophoresis analysis of polymerase chain reaction-amplified genes coding for 16S rRNA. *Appl Environ Microbiol* 59: 695-700

Muraleedharan PM, PrasannaKumar S (1996) Arabian Sea upwelling-A comparison between coastal and open ocean regions. *Curr Sci* 71(11): 842-846

Naqvi SWA, Noronha RJ, Somasundar K, Sen Gupta R (1990) Seasonal changes in the denitrification regime of the Arabian Sea. *Deep-Sea Res I* 37: 593-611

Naqvi SWA, Shailaja MS (1993) Activity of the respiratory electron transport system and respiration rates within the oxygen minimum layer of the Arabian Sea. *Deep-Sea Res II* 40: 687-695

Naqvi SWA (1994). Denitrification processes in the Arabian Sea. *Proc Indian Acad Sci* 103: 279-300

Naqvi SWA, Yoshinari T, Jayakumar DA, Altabet MA, Narvekar PV, Devol AH, Brandes JA, Codispoti LA (1998) Budgetary and biogeochemical implication of N₂O isotope signatures in the Arabian Sea. *Nature* 394: 462-464

Naqvi SWA, Jayakumar DA (2000) Ocean biogeochemistry and atmospheric composition: Significance of the Arabian Sea. *Curr Sci* 78: 289-299

Neilson JW, Jordan FL, Maier RM (2013) Analysis of artifacts suggests DGGE should not be used for quantitative diversity analysis. *J Microbiol Methods* 92(3): 256-63

Newell SE, Babbin AR, Jayakumar A, Ward BB (2011) Ammonia oxidation rates and nitrification in the Arabian Sea. *Global Biogeochem Cy* 25: 1-10

Noble RT, Fuhrman JA (1998) Use of SYBR Green I for rapid epifluorescence counts of marine viruses and bacteria. *Aquat Microb Ecol* 14: 113-118

Pitcher A, Villanueva L, Hopmans EC, Schouten S, Reichart GJ, Damsté JSS, (2011) Niche segregation of ammonia-oxidizing archaea and anammox bacteria in the Arabian Sea oxygen minimum zone. *ISME J* 5: 1896-1904

PrasannaKumar S, Prasad TG, (1996) Winter cooling in the northern Arabian Sea. *Curr Sci* 71: 834-841

Prasannakumar S, Ramaiah N, Gauns M, Sarma VVSS, Muraleedharan PM, Raghukumar S, Kumar DM, Madhupratap M (2001) Physical forcing of biological productivity in the Northern Arabian Sea during the northeast monsoon. *Deep-Sea Res II* 48: 1115-1126

Portmann RW, Daniel JS, Ravishankara AR (2012). Stratospheric ozone depletion due to nitrous oxide: influences of other gases. *Phil Trans R Soc B* 367: 1256-1264

Porter KG, Feig YS (1980) The use of DAPI for identifying and counting aquatic microflora. *Limnol Oceanogr* 25: 943-948.

Ramaiah N, Raghukumar S, Gauns M (1996) Bacterial abundance and production in the central and eastern Arabian Sea. *Curr Sci* 71: 878-882

Ramaiah N, Sarma VVSS, Gauns M, Kumar MD, Madhupratap M (2000) Abundance and relationship of bacteria with transparent exopolymer particles during the 1996 summer monsoon in the Arabian Sea. *Proc Indian Acad Sci (Earth and Planetary Science)* 109: 443-451

Ramaiah N, Raghukumar S, Mangesh G, Madhupratap M (2005) Seasonal variations in carbon biomass of bacteria, thraustochytrids and microzooplankton in the Northern Arabian Sea. *Deep-Sea Res II* 52: 1910-1921

Ramaiah N, Fernandes V, Rodrigues VV, Paul JT, Gauns M 2009 Bacterioplankton abundance and production in Indian Ocean Regions. In I Wiggert JD, Hood RR, Naqvi SWA, Brink KH, Smith SL (eds) *Indian Ocean biogeochemical processes and ecological variability. Workshop on Sustained Indian*

Ocean Biogeochemical and Ecosystem Research (SIBER). Geophys Monogr Ser 185. American Geophysical Union, USA, p 119-132

Rhodes CJ, Truscott JE, Martin AP, Aach RD (2008) Viral infection as a regulator of oceanic phytoplankton populations. *J Mar Syst* 74: 216-226

Riemann L, Steward GF, Fandino LB, Campbell L, Landry MR, Azam F (1999) Bacterial community composition during two consecutive NE Monsoon periods in the Arabian Sea studied by denaturing gradient gel electrophoresis (DGGE) of rRNA genes. *Deep-Sea Res II* 46: 1791-1811

Santegoeds CM, Ferdelman TG, Muyzer G, de Beer D (1998) Structural and functional dynamics of sulfate-reducing populations in bacterial biofilms. *Appl Environ Microbiol* 64:3731-3739

Sen Gupta R, Sankaranarayanan VN, De Sousa SN, Fondekar SP (1976) Chemical oceanography of the Arabian Sea. Part III. Studies on nutrient fractions and stoichiometric relationships in the northern and the eastern basins. *Ind J Mar Sci* 5: 58-71

Simon M, Cho BC, Azam F (1992) Significance of bacterial biomass in lakes and the ocean - Comparison to phytoplankton biomass and biogeochemical implications. *Mar Ecol Prog Ser* 86: 103-110

Singh SK, Ramaiah N (2011) Denaturing gradient gel electrophoresis profiling of bacterial communities composition in Arabian Sea. *J Environ Biol* 32: 339-346

Smith SL, Codispoti LA, Morrison JM, Barber RT (1998) The 1994-1996 Arabian Sea expedition: an integrated interdisciplinary investigation of the northeastern Indian Ocean to monsoonal forcing. *Deep-Sea Res II* 45: 1905-1915

Strom SL (2008) Microbial Ecology of Ocean Biogeochemistry: A Community Perspective. *Science* 320: 1043-1045

Stewart FJ, Ulloa O, DeLong EF (2012) Microbial metatranscriptomics in a permanent marine oxygen minimum zone. *Environ Microbiol* 14: 23-40

Stevens H, Ulloa O (2008). Bacterial diversity in the oxygen minimum zone of the eastern tropical South Pacific. *Environ Microbiol* 10: 1244-1259

ter Braak CJF (1986) Canonical correspondence analysis: a new eigenvector technique for multivariate direct gradient analysis. *Ecology* 67: 1167-1179

Wilhelm SW, Suttle CA (1999) Viruses and nutrient cycles in the sea-viruses play critical roles in the structure and function of aquatic food webs. *Bioscience* 49: 781-788

Wyrtki K (1966) Oceanography of the eastern Pacific Ocean. *Oceanogr Marine Biol Ann Rev* 4: 33-68

Wyrtki K (1973) Physical oceanography of the Indian Ocean. In: Zeitzschel B (ed) *The Biology of the Indian Ocean*. Berlin, Germany, Springer, p 18-36

Zaikova E, Walsh DA, Stilwell CP, Mohn WW, Tortell PD, Hallam SJ (2010) Microbial community dynamics in a seasonally anoxic fjord: Saanich Inlet, British Columbia. *Environ Microbiol* 12: 172-191

Table captions

Table 1. Temporal variations in different physicochemical parameters at the ASTS location during SIM (May, 2012), FIM (September, 2012) and NEM (February, 2013) respectively. TOC values shown here are taken from the data obtained earlier from cruises TTN043 (NEM; Jan, 1995), TTN-045 (SIM; March, 1995), and TTN-50J (FIM; August, 1995) of the Joint Global Ocean Flux Study (JGOFS) Arabian Sea Process Study (ASPS).

Table.2. OTUs richness (S), Shannon diversity index (H') and Pielou's evenness index (J') determined from DGGE profiles of bacterial communities at ASTS

Table 3. Eigenvalues and variance decomposition for CCA in bacterial community samples of ASTS

Table .4 Sequence analyses of DGGE bands. Note that 'B' stands for DGGE band.

Figure captions

Figure 1. Sampling location in the Arabian Sea (A). The 0.5 μM contour marks the boundary of oxygen minimum zone (Naqvi & Shailaja, 1993). Inset shows the vertical section of nitrate and nitrite concentrations from cruise TTN043 of the Joint Global Ocean Flux Study (JGOFS) Arabian Sea Process Study (ASPS) (After Codispoti et al. 2001). The dot lines in the inset mark the ASTS station.

Figure 2. Total bacterial counts (TBC) [closed circle (\bullet)], viral-like particles (VLP) [open circle (\circ)] and virus: bacteria ratio [open square (\square)] at ASTS station during (A) spring Intermonsoon (SIM), (B) fall intermonsoon (FIM), and (C) Northeast Monsoon (NEM).

Figure 3. Cluster analysis of DGGE profiles using group-average linking method. SIMPROF forms two statistically significant groups (represented by black line), Group-I: OMZ group and Group-II: Surface group. Negative image of an ethidium bromide stained DGGE gel shown at right side of the figure. The numbered bands were excised, cloned and sequenced

Figure 4. Linkage tree analysis (LINKTREE) showing clustering of samples based on bacterial community composition and the environmental variables. Note that split B separates surface BC from that of the OMZ due to DO, TOC, nitrate, and silicate. The grey circles represent the samples from group I (OMZ).

Figure 5. Canonical correspondence analysis (CCA) ordination diagram of bacterial communities associated with environmental variables. Environmental variables were indicated as arrows. The first and second ordination axes of CCA, accounted for 21.6% and 9.6% of the explained total variance, respectively. The grey circles represent the samples from group I (OMZ) and the samples from group II are well dispersed in the ordination space.

Figure 6. Phylogenetic tree (maximum likelihood) of V3 region of bacterial 16S rRNA gene amplified using DGGE specific primers, showing the affiliation with database sequences. Bootstrap values $> 50\%$ are given at the nodes (calculated with the neighbour-joining method). The scale bars indicate the percentage of the sequence divergence.

Table 1. Temporal variations in different physicochemical parameters at the ASTS location during SIM (May, 2012), FIM (September, 2012) and NEM (February, 2013) respectively. TOC values shown here are taken from the data obtained earlier from cruises TTN043 (NEM; Jan, 1995), TTN-045 (SIM; March, 1995), and TTN-50J (FIM; August, 1995) of the Joint Global Ocean Flux Study (JGOFS) Arabian Sea Process Study (ASPS).

Parameters	Season	Depths				
		Surface	DCM	250m	500m	1000m
Temperature °C	SIM	30.1989	27.048	18.2419	12.9635	8.6459
	FIM	27.7413	25.8991	16.0034	12.0265	10.2973
	NEM	25.8758	25.6617	15.2883	12.1174	8.5917
Salinity	SIM	36.317	36.358	35.729	35.717	35.341
	FIM	36.519	36.438	36.087	35.616	35.512
	NEM	36.652	36.603	35.750	35.600	35.312
DO (µM/L)	SIM	199.998	203.762	11.794	4.588	9.491
	FIM	205.977	149.308	3.471	0.765	3.066
	NEM	206.627	202.649	1.400	1.510	9.109
pH	SIM	7.93	8.05	7.76	7.59	7.52
	FIM	8.02	8.04	7.22	7.19	7.158
	NEM	8.10	8.22	7.51	7.43	7.31
Nitrate (µM/L)	SIM	ND	0.113	22.417	15.335	38.916
	FIM	ND	8.149	25.002	32.797	38.28
	NEM	0.006	13.376	19.055	25.983	32.897
Nitrite (µM/L)	SIM	0.094	0.071	0.013	0.002	0.08
	FIM	ND	0.295	ND	ND	ND
	NEM	0.043	0.116	2.576	0.058	0.074
Phosphate (µM/L)	SIM	0.235	0.248	2.003	1.600	2.692
	FIM	0.415	0.790	2.35	2.55	2.92
	NEM	ND	0.622	2.227	2.586	3.16
Silicate (µM/L)	SIM	3.077	4.087	18.475	19.441	66.554
	FIM	0.627	2.344	21.793	34.993	50
	NEM	2.903	7.715	29.365	50.296	100.373
Ammonia (µM/L)	SIM	0.009	0.137	0.095	1.008	0.133
	FIM	0.24	0.27	0.19	0.27	0.17
	NEM	ND	0.538	ND	ND	ND
TOC (µM/L)	SIM	83.8	79	54.2	47.8	44.7
	FIM	77.2	71.98	52.43	43.36	43.01
	NEM	69.5	67.9	45.3	38.2	38

ND = Not detected

Table 2. OTUs richness (S), Shannon diversity index (H') and Pielou's evenness index (J') determined from DGGE profiles of bacterial communities at ASTS

Parameters	Season	Depths				
		Surface	DCM	250m	500m	1000m
OTU richness (S)	SIM	8	10	6	6	7
	FIM	7	8	7	5	5
	NEM	9	9	7	6	4
Shannon diversity index (H')	SIM	1.55	2.08	1.52	1.64	1.55
	FIM	1.57	1.9	1.64	1.43	1.18
	NEM	1.81	1.73	1.68	1.45	1.12
Pielou evenness index (J')	SIM	0.56	0.9	0.85	0.79	0.76
	FIM	0.81	0.91	0.79	0.89	0.74
	NEM	0.82	0.79	0.87	0.82	0.81

Table 3. Eigen values and variance decomposition for CCA in bacterial community of ASTS

Axes	Eigenvalues	Cumulative percentage variance of species data	Cumulative percentage variance of species–environment relation	Species–environment Correlations
Axis 1	0.409	21.7	38.7	0.956
Axis 2	0.198	32.2	57.5	0.886
Axis 3	0.141	39.76	70.99	0.832
Axis 4	0.110	45.6	81.4	0.850

Table 4. Sequence analyses of DGGE bands. Note that ‘B’ stands for the DGGE band.

Band no.	Accession no.	Phylogenetic affiliation	Closest relative	Sim (%)	Environmental description
B1	KF724062	<i>Cyanobacteria</i>	Uncultured <i>Prochlorococcus</i> sp. clone 2 (JN547438.1)	99	Subsurface seawater from Red Sea
B2	KF724063	<i>Cyanobacteria</i>	Uncultured <i>Synechococcus</i> sp. clone 031806#33 (FJ903268.1)	99	Seawater from subtropical Kuroshio current
B3	KF724064	<i>Cyanobacteria</i>	Uncultured <i>Prochlorococcus</i> sp. clone BIOS04_GYR_180m 162 (HQ233029.1)	100	Subsurface seawater from central gyre Pacific Ocean
B4	KF724065	<i>Cyanobacteria</i>	Uncultured <i>cyanobacterium</i> clone SWB9B1-04 (KF583385.1)	100	Seawater ballast collected from a transoceanic-bulk carrier vessel
B5	KF724066	<i>Cyanobacteria</i>	Uncultured <i>cyanobacterium</i> clone SWB9A1-41 (KF583342.1)	99	Seawater ballast collected from a transoceanic-bulk carrier vessel
B6	KF724067	<i>Bacteroidetes</i>	Uncultured <i>Flavobacterium</i> sp. clone IMS3D103 (JN233087.1)	99	Surface seawater from Coastal North Carolina, Beaufort Inlet
B7	KF724068	<i>Alphaproteobacteria</i>	Uncultured <i>Sphingopyxis</i> sp. clone C146500352 (JX531372.1)	100	Seawater from southern ocean
B8	KF724069	<i>Gammaproteobacteria</i>	<i>Pseudoalteromonas</i> sp. IMCC17052 (KC593294.1)	99	Seawater from Yellow Sea
B9	KF724070	<i>Alphaproteobacteria</i>	Uncultured <i>Roseobacter</i> sp. clone C146Chl417 (JX530172.1)	100	Subsurface seawater from Southern Ocean
B10	KF724071	<i>Alphaproteobacteria</i>	Uncultured SAR11 cluster <i>alphaproteobacterium</i> clone SWB9A1-11 (KF583294.1)	99	Seawater ballast collected from a transoceanic-bulk carrier vessel
B11	KF724072	<i>Alphaproteobacteria</i>	Uncultured SAR11 cluster alpha proteobacterium clone SWB9B1-114 (KF583332)	96	Seawater ballast collected from a transoceanic-bulk carrier vessel
B12	KF724073	<i>Alphaproteobacteria</i>	Alpha proteobacterium SCGC AAA300-J04 (HQ675313.1)	100	Subsurface seawater from HOT Station ALOHA North pacific subtropical gyres
B13	KF724074	<i>Alphaproteobacteria</i>	Uncultured <i>alphaproteobacterium</i> clone 422-47 (JQ772381.1)	98	Seawater from northern South China Sea
B14	KF724075	<i>Alphaproteobacteria</i>	Uncultured bacterium clone CART_E6 (JX455720.1)	98	Symbiotic bacteria in Great Barrier Reef sponges
B15	KF724076	<i>deltaproteobacteria</i>	Uncultured Desulfobacterales bacterium clone HF770_28H03 EU361110.1	98	Deep seawater from HOT Station ALOHA North pacific subtropical gyres
B16	KF724077	<i>Gammaproteobacteria</i>	<i>Idiomarina</i> sp. SN-14 strain SN-14 (HF954116)	98	Sewater from solar saltern in Huelva, Spain
B17	KF724078	<i>Alphaproteobacteria</i>	Uncultured SAR11 cluster <i>alphaproteobacterium</i> clone F9P4_10L02 (HQ242265.1)	100	Seawater from North East Pacific
B18	KF724079	<i>betaproteobacteria</i>	Uncultured beta proteobacterium clone URO127.E12 (JX473166.1)	100	Fresh water lake Baikal
B19	KF724080	<i>Gammaproteobacteria</i>	Uncultured <i>gammaproteobacterium</i> clone JL-ETNP-S59 (AY726870)	100	Seawater from Eastern Tropical North Pacific Ocean
B20	KF724081	<i>Gammaproteobacteria</i>	Uncultured <i>gammaproteobacterium</i> clone (JN388027.1)	95	Ianthella basta bacterial symbiont

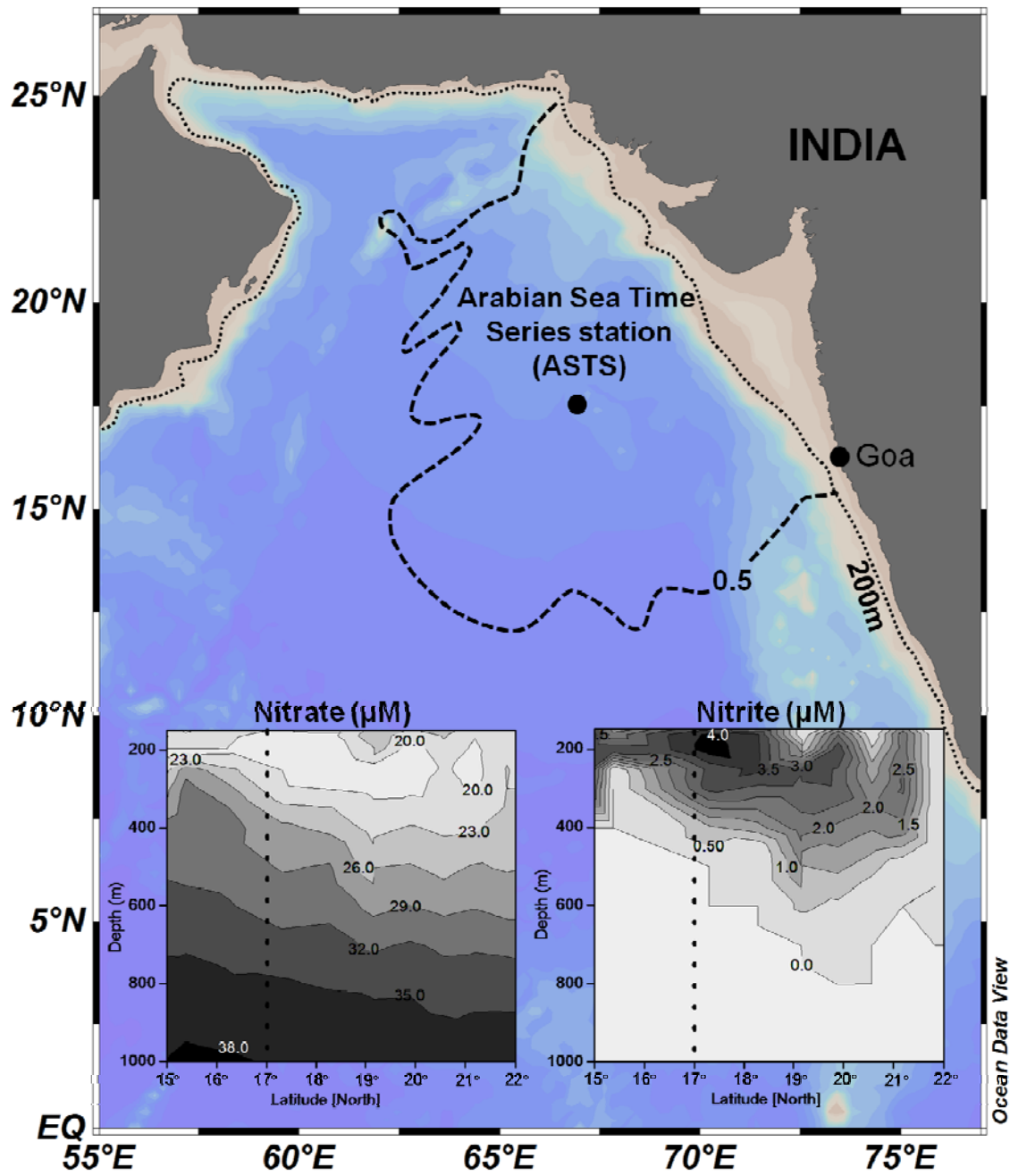


Figure 1. Sampling location in the Arabian Sea. The 0.5 μM contour marks the boundary of oxygen minimum zone (Naqvi & Shailaja, 1993). Inset shows the vertical section of nitrate and nitrite concentrations from cruise TTN043 of the Joint Global Ocean Flux Study (JGOFS) Arabian Sea Process Study (ASPS) (After Codispoti et al. 2001). The dot lines in the inset mark the ASTS station.

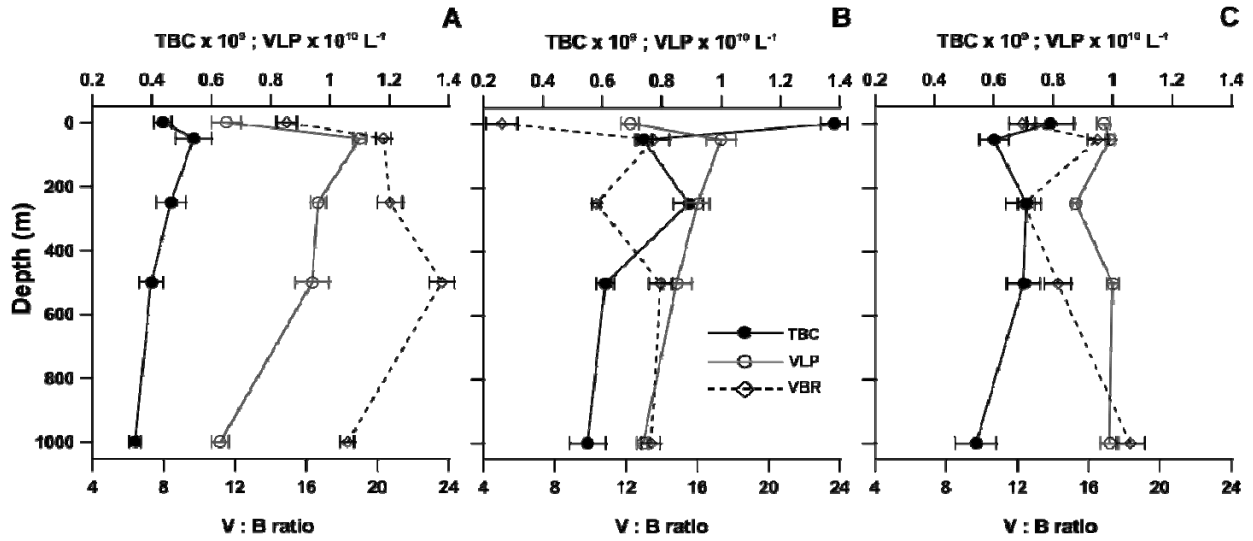


Figure 2. Total bacterial counts (TBC) [closed circle (●)], viral-like particles (VLP) [open circle (○)] and virus: bacteria ratio [Open Square (□)] at ASTS station during (A) spring Intermonsoon (SIM), (B) fall intermonsoon (FIM), and (C) northeast monsoon (NEM).

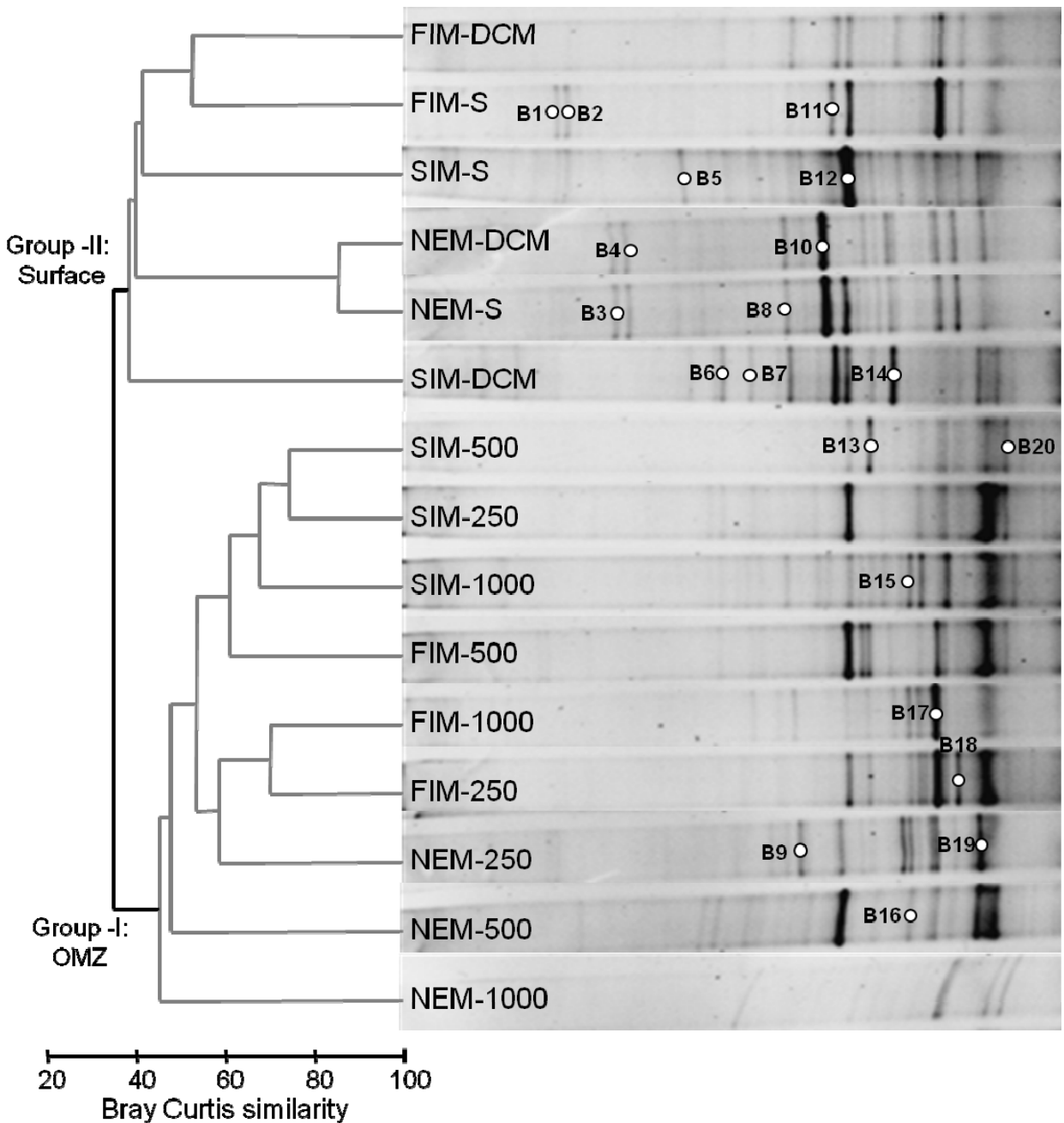


Figure 3. Cluster analysis of DGGE profiles using group-average linking method. SIMPROF forms two statistically significant groups (represented by black line), Group-I: OMZ group and Group-II: Surface group. Negative image of an ethidium bromide stained DGGE gel shown at right side of the figure. The numbered bands were excised, cloned and sequenced

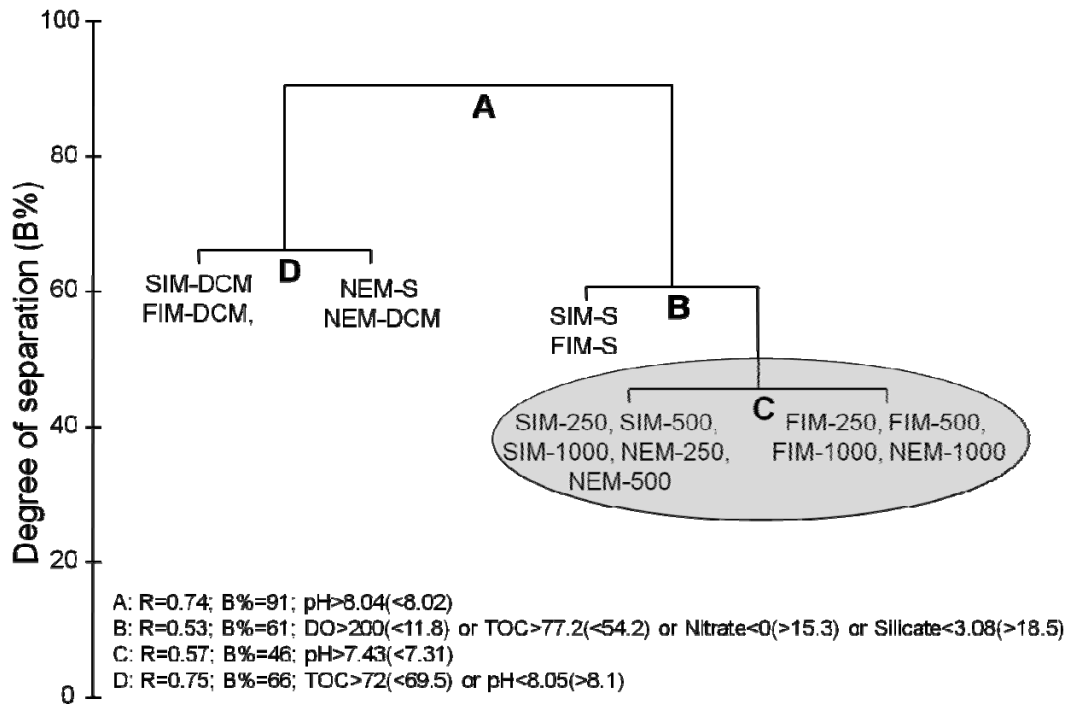


Figure 4. Linkage tree analysis (LINKTREE) showing clustering of samples based on bacterial community composition and the environmental variables. Note that split B separates surface BC from that of the OMZ due to DO, TOC, nitrate, and silicate. The grey circles represent the samples from group I (OMZ).

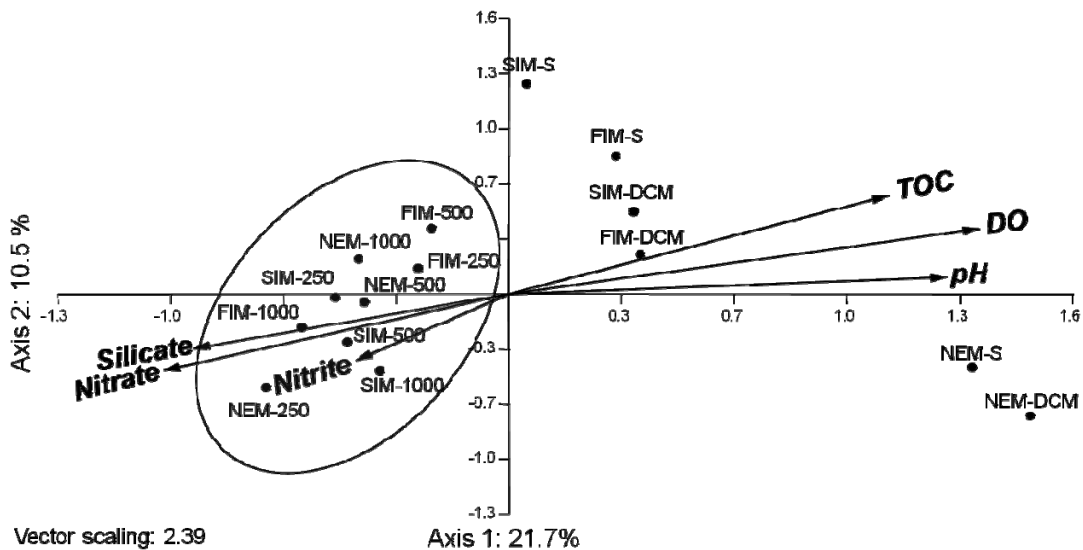


Figure 5. Canonical correspondence analysis (CCA) ordination diagram of bacterial communities associated with environmental variables. Environmental variables were indicated as arrows. The first and second ordination axes of CCA, accounted for 21.6% and 9.6% of the explained total variance, respectively. The grey circles represent the samples from group I (OMZ) and the samples from group II are well dispersed in the ordination space.

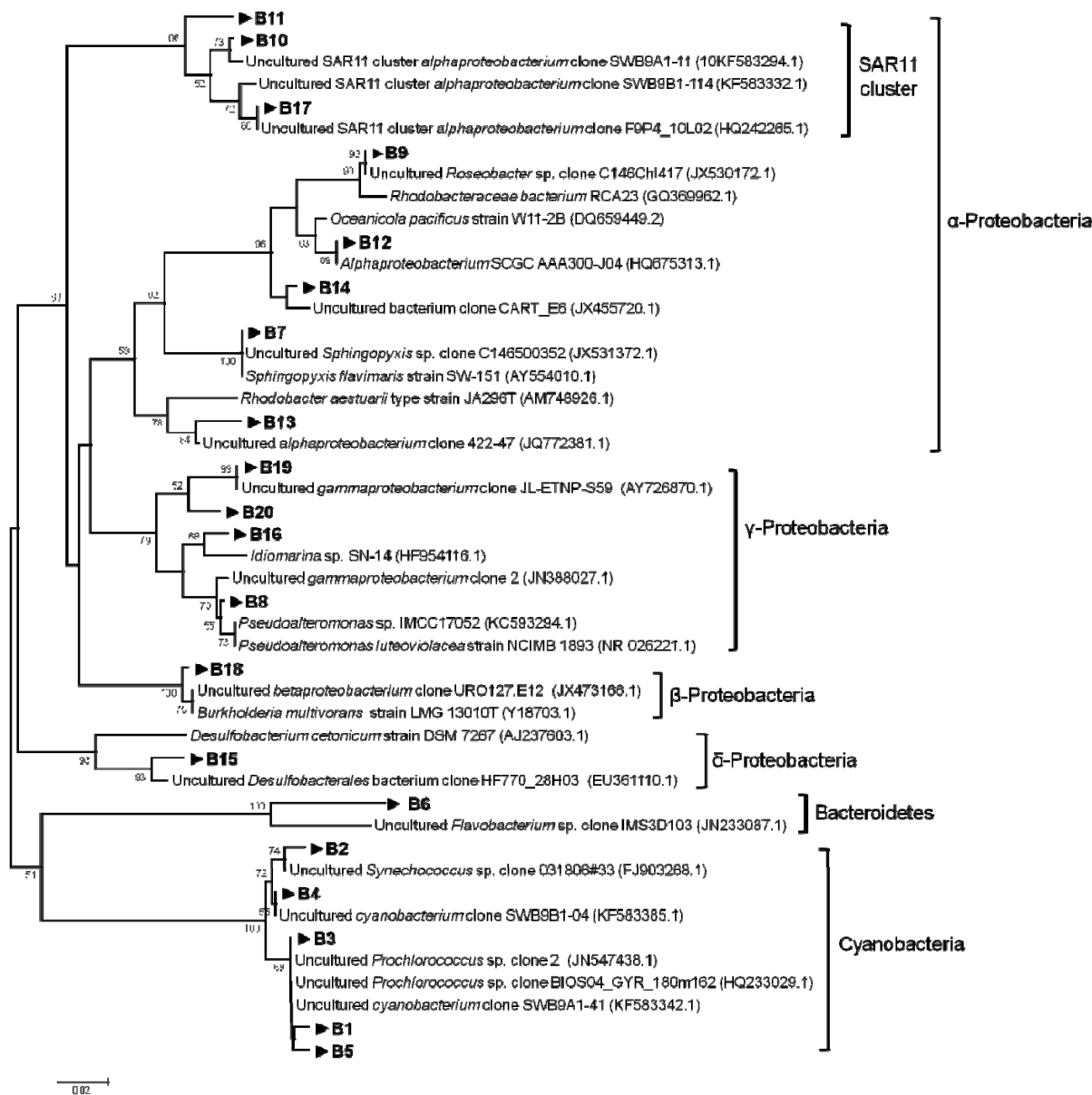


Figure 6. Phylogenetic tree (maximum likelihood) of V3 region of bacterial 16S rRNA gene amplified using DGGE specific primers, showing the affiliation with database sequences. Bootstrap values > 50% are given at the nodes (calculated with the neighbour-joining method). The scale bars indicate the percentage of the sequence divergence.

Supplementary Figure

Supplementary figure captions

Figure S.1. Non-metric multidimensional scaling (NMDS) plot of DGGE profile based on relative intensity of bands using Bray- Curtis similarity index, the samples within the complete and dotted circle are 35% and 45 % similar in bacterial community (BC) structure, respectively. The grey circle represents the OMZ group.

Figure S.2. Bacterial community structures during SIM, FIM and NEM seasons based on the quantitative analysis of the DGGE bands.

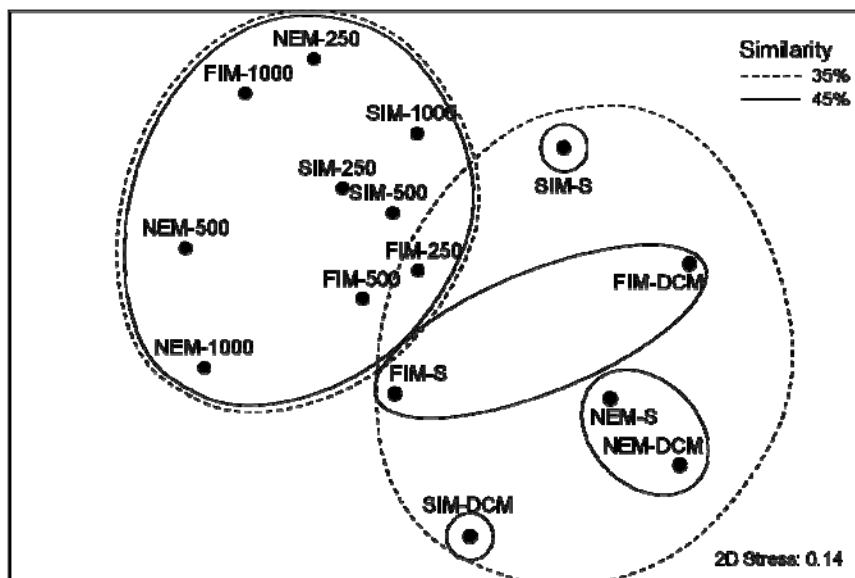


Figure S.1. Non-metric multidimensional scaling (NMDS) plot of DGGE profile based on relative intensity of bands using Bray- Curtis similarity index, the samples within the complete and dotted circle are 35% and 45 % similar in bacterial community (BC) structure, respectively. The grey circle represents the OMZ group.

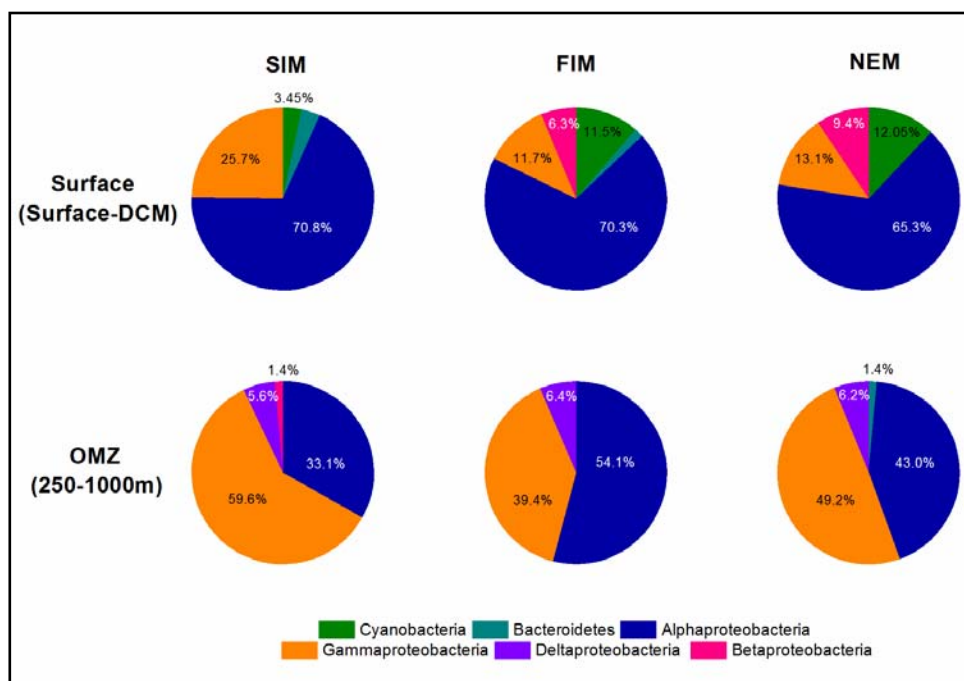


Figure S.2. Bacterial community structures during SIM, FIM and NEM seasons based on the quantitative analysis of the DGGE bands.